https://doi.org/10.5194/se-2020-175
Preprint. Discussion started: 19 October 2020
© Author(s) 2020. CC BY 4.0 License.

Solid Earth
Discussions
Open Access
EGU

Kinematics of subduction in the Ibero-Armorican arc constrained by 3D microstructural analysis of garnet and pseudomorphed lawsonite porphyroblasts from Ile de Groix (Variscan belt)

Domingo G.A.M. Aerden[a,b]

Mohammad Sayab[d]

Aidan Forde[c]

Alejandro Ruiz-Fuentes[a]

[a]Departamento de Geodinámica, Universidad de Granada, Spain

[b]Instituto Andaluz de Ciencias de la Tierra, CSIC/Universidad de Granada, Spain

[c]Saorgus Energy Ltd, Kerry, Ireland

[d]Geological Survey of Finland, Espoo, Finland

Abstract

The small island of Groix in southern Brittany, France, is well known for its excellent outcrops of Variscan blueschists, eclogites and garnetiferous micaschists that define a Late-Devonian suture between Gondwana and Armorica. The kinematics of polyphase deformation in these rocks is reconstructed based on 3D microstructural analysis of inclusion trails in garnet- and pseudomorphed lawsonite porphyroblasts using multiple, differently oriented thin sections of single samples and X-ray tomography. Three sets of inclusion trails striking NE-SW, NNW-SSE and WNW-ESE are interpreted to witness a succession of different crustal shortening directions orthogonal to these trends. The curvature sense of sigmoidal- and spiral-shaped inclusion trails of the youngest set is shown to be consistent with southward thrusting or northward subduction of Gondwana under Armorica, provided that these microstructures developed by overgrowth of actively forming crenulations instead of the previously envisaged 'snowball' mechanism. The latter predicts an opposite thrusting direction which is at odds with the regional tectono-metamorphic zonation in the Ibero-Armorican Arc. Strongly non-

https://doi.org/10.5194/se-2020-175
Preprint. Discussion started: 19 October 2020
© Author(s) 2020. CC BY 4.0 License.

Solid Earth
Discussions
Open Access
EGU

cylindrical folds locally found on Ile de Groix are reinterpreted as fold-interference structures instead of having formed by progressive shearing. Six additional samples of lower-grade footwall units of the Groix ophiolite were also studied. The oldest inclusion trails in these rocks have similar trends as the youngest one in Ile de Groix. Our new inclusion-trail data for southern Brittany bear a strong resemblance with those documented previously in the north-western Iberian Massif and suggest about 20° clockwise rotation of Iberia during the early Cretaceous opening of the Gulf of Biscay.

Key words: porphyroblast inclusion trails, FIA, Variscan subduction, Ibero-Armorican arc, Ile de Groix.

1. Introduction

Kinematic reconstructions in polydeformed metamorphic regions are traditionally based on a combination of geological mapping, study of structural relationships in outcrop, orientation measurements, and study of thin sections usually cut parallel to the stretching lineation to determine a shear sense. Not rarely does this approach produce paradoxical data that insufficiently constrain different possible tectonic models as is certainly the case of Ile de Groix as we will see. However, following a major conceptual shift concerning the formation mechanism and tectonic significance of porphyroblast inclusion trails (Bell et al., 1985, 1986; Bell & Johnson, 1989), 3D microstructural data for such microstructures has been shown to allow detailed reconstruction of deformation histories whose complexity was previously not recognized. Aerden (2004) pioneered this approach in Variscan NW Iberia in a research project led by José Ramón Martínez Catalán. He distinguished 4 inclusion-trail sets with specific, regionally consistent trends and relative timing. An E-W trend of the earliest formed set was interpreted to record N-S directed compression and subduction with unknown polarity. Subduction would have been followed by several changes in the direction of crustal shortening responsible for the 3 younger sets of inclusion trails. The youngest two sets with NE-SW and WNW-ESE trends were correlated with regional-scale fold-interference patterns developed throughout the Iberian Massif and this, in turn, was key to rediscovering a partially blind arc in central Iberia later endorsed by Martinez Catalán et al. (2012).

Here, we report a similar study of inclusion trails in the Armorican Massif focusing on high-pressure metabasites of Ile de Groix, but also including data from lower-grade rocks located in their footwall. The island of Groix (ca. 15 km^2) is a national reserve with excellent

https://doi.org/10.5194/se-2020-175
Preprint. Discussion started: 19 October 2020
© Author(s) 2020. CC BY 4.0 License.

Solid Earth
Discussions
Open Access
EGU

coastal outcrops of Variscan blueschists, eclogites and interlayered garnetiferous micaschists that are generally accepted to represent the remains of a narrow ocean that, in the late Silurian and lower Devonian separated Gondwana in the south from the Armorica microplate to the north. In NW-Iberia, a similar ophiolitic unit is since long recognized and correlated with the one exposed on Groix island (Arenas et al., 1995; Diaz-García et al., 1999; Ballèvre et al., 2009, 2015). Closure of this ocean involved subduction of the margin of Gondwana causing high-pressure metamorphism dated 370-360Ma on Ile de Groix (Bosse et al., 2005). However, the polarity and kinematics of ophiolite emplacement have remained poorly constrained by (micro)structural data. Indeed, not much has changed since Quinquis et al. (1978) wrote: "*the bulk sense of shear on Groix has not yet been determined unequivocally, but may perhaps be deduced from systematic analyses of fold asymmetry and of microstructures in and around syntectonic garnets. The significance of glaucophane orientation in the basic rocks of Groix also needs to be studied: the orientation is extremely variable and may not be simply related to a shear direction.*" Exactly along these lines of suggested further research, we performed a detailed microstructural analysis of 10 garnetiferous blueschist samples of Ile de Groix, 4 samples of albite-porphyroblast bearing greenschists (Pouldu schists) cropping out along the coast of the mainland, and 2 kyanite-staurolite schists collected inland from the North-Armorican Zone (Fig. 1). It will be shown that behind the simple appearance of the regional stretching lineation pattern on Ile de Groix, a complex tectonic evolution is hidden recorded by inclusion trails in garnets and pseudomorphed lawsonite crystals. Our microstructural data resolve conflicting kinematic interpretations of previous workers regarding and proposes a new polyphase model for sheath folds locally found on the island.

2. Geological setting and previous work

The Variscan (or Hercynian) orogeny took place in the Devonian and Carboniferous as a consequence of Gondwana-Laurussia convergence with 2 microcontinents in between these 2 giants known as Armorica and Avalonia. The resulting closure of oceanic domains created multiple ophiolitic sutures whose precise location, timing and correlation continues to be a major research topic (e.g. Azor et al., 2008; Faure, 2008; Ballèvre et al., 2009; Arenas et al., 2016). The high-pressure rocks of Ile de Groix are part of a partially submerged ophiolitic klippen belonging to a thrust nappe that separates Armorican crustal units in the hangingwall outcropping to the North- and Central Armorican Domains, from North-Gondwana derived crustal units below the suture outcropping in the South Armorican Domain and NW Iberia

https://doi.org/10.5194/se-2020-175
Preprint. Discussion started: 19 October 2020
© Author(s) 2020. CC BY 4.0 License.

Solid Earth
Discussions
Open Access
EGU

(Fig. 1). Because of this regional-scale zonation, a north-dipping subduction zone associated with south verging thrusts has been considered the most likely geodynamic scenario (Matte, 2001; Faure et al., 2008; Ballèvre et al., 2009; Ballèvre 2015). However, structural data have not allowed to independently confirm this model and in fact have yielded conflicting results.

Lagarde (1980) concluded NW directed thrusting from shear criteria in the Champtoceaux Complex (Fig. 1), implying south-east subduction. A similar kinematic was deduced on Ile de Groix by Quinquis (1980), Quinquis & Choukroune (1981) and Cannat (1985) from rotated snowball garnets and quartz c-axes fabrics. Recognizing the conflict with respect to northward subduction, these authors proposed that this shear sense corresponds to backthrusting and obduction of ophiolites in opposite direction as subduction.

However, Quinquis (1980) noticed that shear bands (C and C' planes) on Ile de Groix indicate opposite shear senses, which was later interpreted by Shelley and Bossière (1999) in terms of bulk vertical shortening and crustal thinning. These authors emphasized that shear bands showing opposite displacements cannot be linked to different metamorphic conditions and probably formed as conjugate sets. They also found equal amounts of oppositely shear senses indicated by quartz fabrics which they measured in 57 oriented samples. Philippon et al. (2009) argued on the contrary that opposite shear-band sets did form consecutively under different metamorphic conditions. A first set would have developed during prograde metamorphism with top-to-the SW (N140) shearing, and the second during quasi-opposite top-to-the-north (N350) shearing and retrogression. However, they failed to address a top-to-the-north shear sense during prograde metamorphism deduced from rotated garnets by Quinquis & Choukroune (1981).

3. Microstructural methods

A total of 132 oriented thin sections were studied of 33 samples: 20 from Ile de Groix, 9 from the Pouldu schists and equivalent rocks cropping out in the Baye d'Audièrne, and 4 from the Central Armorican Zone (Fig. 1). Initially, a horizontal thin section was cut of each sample to assess the interest of the rock for further study and to measure the strike of inclusion trails. The latter only proved possible in about half of the samples as the other half contained garnets that were too altered or contained poorly developed or absent inclusion trails. Strike measurements for inclusion trails are plotted in moving-average rose diagrams made with the Excel Workbook MARD (Munro & Blenkinsop, 2012).

https://doi.org/10.5194/se-2020-175
Preprint. Discussion started: 19 October 2020
© Author(s) 2020. CC BY 4.0 License.

Solid Earth
Discussions
Open Access
EGU

Seven Ile de Groix samples containing the most promising inclusion trails were further studied in 6 vertical thin sections striking N0, N30, N60, N90, N120 and N150. Such radial thin-section sets allow determination of the average trend of inclusion-trail curvature axes (Hayward, 1990) know as 'FIA' in the more recent literature ('Foliation Intersection- or Inflexion-Axes'; Bell et al., 1992; Bell et al., 1995; Stallard et al., 2003; Kim & Sanislav, 2017). Application of this technique has in numerous mountain belts revealed regionally consistent orientations of FIA (Kim and Sanislav, 2017 and references cited therein) thought to record crustal shortening directions orthogonal to FIA trends and changes therein where multiple sets of FIA can be distinguished.

Four of our Ile-de-Groix samples (G3, G11, G12 and G14) were studied in even greater detail using X-ray computed tomography allowing study if of virtual sections of any orientation and location in a scanned volume, as well as quantitative analysis of mineral-grain shapes.

4. Strike and pitch measurements of inclusion-trails

The samples studied in detail from Ile de Groix come from 3 areas in the north (G18-20), east (G3, G7) and south-east (G11-15) of the island (Fig. 2a). The matrices of these rocks contain a mineral/stretching lineation that exhibits significant variation but overall trends N-S in the south-east of the island changing gradually towards NW-SE towards the north and west. Bosse et al. (2002) inferred a thrust contact separating garnetiferous eclogites, blueschists and micaschists exposed in the eastern half of the island from underlying lower-grade (albite-epidote facies) rocks outcropping in the western half (Triboulet, 1974; Schulz, 2001).

Since stretching lineations on Groix are associated with a foliation that generally dips gently or subhorizontal, shearing-induced rotation of porphyroblasts can be expected to have resulted in inclusion trails that broadly strike orthogonal to the lineation (Fig. 3a). Our measurements, however, show exactly the opposite, a NNE-SSW strike maximum of inclusion trails subparallel to the stretching lineation. This is only a first indication that the classic interpretation of internal foliations based on Zwart (1960), Spry (1963) or Roosenfeld (1970) may be incorrect and that the alternative model proposed by Bell (1985) and Bell et al. (1986) has to be considered. The latter claims that sigmoidal and spiral-shaped inclusion trails form by punctuated overgrowth of one or multiple crenulation cleavages by porphyroblasts that rotate little or not during deformation due to the micro-partitioning of deformation between cleavage planes and microlithons (Fig. 3b). FIAs represent 'fossil' crenulation axes in

https://doi.org/10.5194/se-2020-175
Preprint. Discussion started: 19 October 2020
© Author(s) 2020. CC BY 4.0 License.

Solid Earth
Discussions
Open Access
EGU

this model and this explains why FIA are commonly parallel to crenulation- and fold-axes in the matrix (Aerden, 1995, 2004, 1998, Sayab, 2005, Aerden et al., 2013; Bell & Sanislav, 2011).

Further evidence supporting a 'non-rotational ' origin of sigmoidal and spiral-shaped in Ile de Groix is provided by garnets in samples G7, G11 and G14. These exhibit the same characteristic truncation surfaces that Bell & Johnson (1989) drew attention to. They showed that these truncations in spiral garnets from different orogens systematically align along vertical and horizontal axes, something that has been amply confirmed by later research (e.g. Bell et al., 1992; Hayward, 1992; Aerden, 1994, 1998, 2004; Mares, 1998; Bell & Sapkota, 2012; Sayab, 2005; Shah et al., 2009; Aerden and Ruiz Fuentes, 2020). Oriented line drawings of spiral garnets in G7, G14 and G11 also show orthogonal preferred orientations of their truncations (Fig. 4) in agreement with their origin by stepwise overgrowth of successive subvertical and subhorizontal crenulation cleavages.

5. Curvature sense of inclusion trails

The above mentioned rotational and non-rotational models deduce an opposite shear sense from a given inclusion trail curvature sense. Quinquis & Choukroune (1981) reported that out of a total of 29 thin sections they studied cut parallel to the stretching lineation, 26 contained sigmoidal or spiral-shaped inclusion trails indicating top-to-the north shearing. As they assumed the traditional 'rotational' model, it follows that their inclusion trails predominantly curve anticlockwise when viewed in westward direction. In effect, we found the same predominance in our samples after counting the number of clockwise vs. anticlockwise trails in all vertical thin sections striking N-0, N30, N120 and N150. That is all thin sections making a small angles with the regional stretching lineation. This resulted in 99 anticlockwise and 27 clockwise inclusion trails (viewing westward), a ratio of about 4:1.

According to the 'non-rotational' model, the observed asymmetry, in principle, implies crustal shortening with a component of north-side-up shearing on vertical foliations alternating with gravitational collapse with a component of top-to-the south shearing on horizontal foliations (Bell & Johnson, 1989, their Figs. 16 and 17). Note that this is consistent with the northward subduction interpreted by most authors from the regional tectonometamophic zonation in the Ibero-Armorican Arc. Quinquis & Choukroune (1981), however, deduced an opposite thrusting direction from the same inclusion trails and attempted

https://doi.org/10.5194/se-2020-175
Preprint. Discussion started: 19 October 2020
© Author(s) 2020. CC BY 4.0 License.

Solid Earth
Discussions
Open Access
EGU

to reconcile this with a northward subduction by invoking backthrusting and ophiolite obduction, for which there is little independent evidence.

Strain shadows around porphyroblasts composed of quartz, feldspar and chlorite do not show consistent asymmetries. In fact, they are commonly rather symmetrical or showing opposite asymmetries even on both sides of the same porphyroblast. Where a clear asymmetry is observed it is consistent with the shear sense indicated by inclusion trail curvature according to the non-rotational model only (Figs. 5a, b).

So, we could have finished our paper here with the conclusion that no reconciliation is needed, if not a more detailed 3D study of porphyroblasts had revealed a far more complex tectonic history including different tectonic transport directions associated with multiple inclusion-trail sets and FIA.

6. Average FIAs

Hayward (1990) devised a method for constraining the average trend of porphyroblast FIAs in a sample using a radial set of vertical thin sections in which the asymmetry (i.e. curvature sense) of inclusion trails is recorded. Where the asymmetry flips between two thin sections, the FIA passes between them. We successfully applied the method in 5 Ile de Groix samples, whose average FIAs are shown in Fig. 2b. FIAs are constrained to within 30° trend ranges but 10° for samples G7 from which 2 extra thin sections were cut. Additionally, the plunge direction was determined from the asymmetry of inclusion trails in horizontal thin sections.

In the next section it will be shown that average FIAs can be matched to specific orientation maxima seen in the rose diagrams for inclusion trails strikes (Fig. 2b), although not necessarily the strongest maximum. In sample G12 a correlation is not possible, though, due to large variation of individual FIAs about a mean vector whose trend does not match the strikes of associated inclusion-trails.

No results average FIAs could be determined in samples G18 and G20 as no clear asymmetry switch was observed between the different thin sections. In fact, most thin sections contain inclusion trails showing opposite curvature senses, probably reflecting the presence of more than just one FIA sets in these samples with different orientations. G3, G13 and G15 contained mostly straight inclusion trails and insufficient numbers of asymmetrically curved ones to apply the technique.

https://doi.org/10.5194/se-2020-175
Preprint. Discussion started: 19 October 2020
© Author(s) 2020. CC BY 4.0 License.

Solid Earth
Discussions
Open Access
EGU

7. X-ray tomography

7.1. Sample G11

G11 is a blueschist from 'Amer' in the SE of the island (Fig. 2a). It contains garnet porphyroblasts as well as rectangular pseudomorphs composed of a mixture of white mica, chlorite, albite and epidote after lawsonite probably (Cogné et al., 1966; Felix & Fransolet, 1972; Ballèvre et al., 2003). Lawsonite relics have never been found, though, and some authors have argued that the replaced mineral was plagioclase (Shelley & Bossière, 1999). Lawsonite, as a high-pressure mineral, should have grown partially synchronous with garnet on a prograde path, whereas plagioclase is more likely to have formed during retrogression. G11 therefore provides us with an opportunity to investigate the relative timing of garnet and hence the origin of pseudomorphs from a microstructural perspective.

Inclusion trails in garnet vary from simple to sigmoidal to spiral-shaped but do not curve more than about 90° from the center to the rim (Figs. 5a, b, c, g and 6). We used the *Fiji* image-analysis software (Schindelin et al., 2012) to measure the spatial orientation of relatively straight inclusion-trails or inclusion-trail segments visible in our tomographic scans (Tiff image stacks). This was done by fitting the strike and pitch angles of these elements, measured on 3 mutually orthogonal (virtual) sections, to great circles. The curvature axes of inclusion-trails or 'FIA' were measured using the radial slicing technique detailed in Aerden & Ruiz-Fuentes (2020) which is completely analogous to the thin-section based technique of Hayward (1990) and Bell et al. (1995).

The X-ray scan of G11 revealed the existence of relatively large elongate crystals with high X-ray attenuation (higher than garnet) and hence density, which in section were identified as an Fe-rich opaques, partially or completely replaced by brown-reddish goethite (Fig. 5d, h). Some of these opaques attain porphyroblast sizes and contain scarce inclusion trails. Reflected-light imaging showed that the opaque phase is a mixture of ilmenite and magnetite, the latter possibly replacing the former. The shape orientation of these crystals was characterized by automatic calculation of best-fit ellipsoids using Fiji's *BoneJ* plugin (Doube et al., 2010). Ellipsoid long-axes (X) strongly align with the macroscopic mineral/stretching/intersection lineation, whereas the XY planes lie in the plane of the matrix foliation.

Garnets with sigmoidal- or spiral-shaped inclusion trails in sample G11 were measured both in the center and in the rims where they become strongly deflected or

https://doi.org/10.5194/se-2020-175
Preprint. Discussion started: 19 October 2020
© Author(s) 2020. CC BY 4.0 License.

Solid Earth
Discussions
Open Access
EGU

truncated by younger inclusion trails. The porphyroblast-rim measurements tightly define a steeply SW dipping plane, whereas porphyroblast-core foliations vary significantly from steeply NW dipping to shallowly W-dipping. Intersection lines of core and rim planes measured in the same porphyroblast agree well with the FIAs measured independent by virtual radial-slicing. FIAs dip moderately west in the sample, and confirmed the average FIA trend already deduced from the radial thin sections (Fig. 2b). The orientations measured for simple (straight) inclusion trails coincide with the ones measured in the cores and rims of sigmoidal and spiral-shaped trails, suggesting they represent both microfabrics and grew at different times. Based on the above data we may confidently interpret the bimodal inclusion-trail strikes in the rose diagram for G11 as reflecting the same two sets of inclusion trails with an older NNW-SSW striking and a younger WNW-ESE striking set.

Lawsonite pseudomorphs in G11 also exhibit visible inclusion trails in the X-ray scans (Fig. 5e, f, and h) although these are less finely spaced and well defined as in garnet. These trails have a straight to weakly sigmoidal geometry oblique to the matrix foliation and subparallel to inclusion trails in garnet-rim. This suggests lawsonite growth after garnet cores but synchronous with garnet rims, consistent with previously reported large pseudomorphs sometimes including garnet (e.g. Ballèvre et al., 2003). Significantly, the asymmetry or curvature sense of inclusion trails in the pseudomorphs is opposite as in garnets when viewed in a N-S vertical sections. This implies a component of top-to-the-S shearing during the growth of porphyroblast cores, followed by top-to-the-N shearing when the garnet rims and lawsonite developed. Interestingly, Philippon et al. (2009) proposed the same shear-sense reversal (top-to-N140, then top-to-N350) from different sets of shear bands in the area of Amer, but note that their interpretation is only compatible with the observed inclusion-trail curvature senses if one accepts a 'non-rotational' origin.

7.2. Sample G12

G12 is a similar blueschist as G11 from the same outcrop but no lawsonite pseudomorphs were found in it. The tomographic data for this sample reveals an early NNW-SSE striking foliation preserved in porphyroblast cores and as simple inclusion trails, overprinted by a steeply S-dipping foliation preserved in garnet rims. The garnet-rim foliation is in turn deflected or truncated by a subhorizontal crenulation cleavage that causes transposition in the matrix and constitutes the composite 'main foliation'. The same opaque minerals as described in G11 are also present with the difference that now also occur as large

https://doi.org/10.5194/se-2020-175
Preprint. Discussion started: 19 October 2020
© Author(s) 2020. CC BY 4.0 License.

Solid Earth
Discussions
Open Access
EGU

inclusions within garnets, often occupying a central position suggesting that the garnets nucleated on those grains. Opaques in the matrix are strongly elongated NW-SE subparallel to the strike of inclusion trails in the garnets.

The above data allow confident correlation of the different peaks in the strike rose diagrams for G11 and G12 in Fig. 2b. These peaks correspond to (1) an early NE-SW striking foliation preserved in the cores of spiral-shaped inclusion trails, (2) a younger NNW-SSE striking foliation included in the cores of sigmoidal inclusion trails with variable dip angles, and (3) a still younger ESE-WNW foliation preserved in garnet rims and in lawsonite pseudomorphs. Note however that the average FIA trends determined for both samples are quite different falsely suggesting they record different deformation histories. This difference results from the variable dip angles of inclusion trails sharing the same strike and relatively steep plunges of FIAs.

7.3. Sample G14

G14 is another blueschist sample from Amer that contains numerous relatively small (1-2 mm) garnets with straight, sigmoidal or spiral-shaped inclusion-trails. The spiral patterns exhibit significantly greater curvature (up to 180°; Fig. 4b) as in G11 and G12. Unfortunately, only a few garnets had visible inclusion trails in the tomographic scan because of their very fine grain size and profuse fracturing of garnets. A few inclusion-trail planes could be measured plus 5 FIAs that plunge steeply in different directions (Fig. 7a).

The same elongate opaque crystals as found in G3, G11 and G12 are also present aligned with the macroscopic stretching/mineral lineation. Their XY planes (normal to Z) have variable dips but consistent N to NE strike parallel to that of most inclusion-trails (Fig. 2b). An interesting fold structures outlined by an epidote-rich layer was found whose axial trace also trends NE-SW suggesting a genetic link with the inclusion trails further supported by the available 3D data (Fig. 7a). E-W sections through the fold (Fig. 7c) show its refolding with subhorizontal axial suggesting subvertical shortening and probably related to the horizontal crenulation cleavage in G7 (Fig. 4a). In plan view the fold is transected by N-S striking cleavage zones also outlined by irregularly folded quartz lenses (Fig. 7d).

7.4. Sample G3

https://doi.org/10.5194/se-2020-175
Preprint. Discussion started: 19 October 2020
© Author(s) 2020. CC BY 4.0 License.

Solid Earth
Discussions
Open Access
EGU

G3 was collected close to Fort Nosterven on the east coast of the island, about 1 km south of Plage du Trech. Garnets in this glaucophane-epidote schist have well developed straight and sigmoidal inclusion trails whose strikes were measured in thin section. Unfortunately, the trails were poorly visible in the tomographic scan. The few that could be measured dip steeply NW, similar as the inclusion trails in garnet cores of samples G11 (Fig. 8a; compare with Fig. 6). A correlation is also likely with the average FIA determined in sample G7 (collected a bit further north at Plage du Trech) and gently SSW plunging fold axes measured there by Audren (1974, unpublished data; Fig. 8b). One individual garnet FIA defined by sigmoidal inclusion trails could be constrained by virtual radial slicing. Inclusion-trails in the rim of this porphyroblast are approximately subvertical with N120 strike and hence can be correlated with inclusion trails in the garnet rims in G11 and G12.

8. Interpreted deformation history

The above microstructural data lead us to interpret a succession of 3 shortening directions that produced 3 sets of steeply dipping inclusion trails associated with different strike maxima. The preservation of their original orientations was possible due to non-rotational behavior of porphyroblasts. These foliations could may have alternated with subhorizontal ones related to intermitted gravitational collapse stages, but the predominantly moderate to steep plunges of FIAs in the samples studied with X-ray tomography suggests these events were in any case weak. Otherwise, predominantly subhorizontal FIA plunges would be expected (cf. Bell et al., 2005; Aerden & Ruiz-Fuentes, 2020). The latest subhorizontal cleavage however developed penetratively and caused extensive transposition earlier steep fabrics and related upright folds. The growth of garnet rims and lawsonite porphyroblasts was probably triggered by incipient development stages of this foliation (cf. Bell & Hayward, 1991*) but would have ceased soon afterwards as the rocks were exhumed.

The earliest formed steep foliation with NE-SW strike preserved in G3, G11 and G14 corresponds to orthogonal SE-NW crustal shortening. This early foliation was reoriented and modified in the matrix during the development of a younger N-S to NNE-SSW striking foliation. Its intersection with the pre-existing NE-SW foliation explains the steeply dipping FIA measured in G14. This event corresponded to ENE-WSW directed compression. A third steeply foliation dipping steeply south with E-W to WNW-strike is preserved in garnet rims and as simple inclusion trails in G11 and G12, as well as in lawsonite pseudomorphs of G11. It was created during N-E to NNE-SSW compression close to peak-metamorphic conditions

https://doi.org/10.5194/se-2020-175
Preprint. Discussion started: 19 October 2020
© Author(s) 2020. CC BY 4.0 License.

Solid Earth
Discussions
Open Access
EGU

as this is when lawsonite is likely to have formed (Ballèvre et al., 2003). The presence of this foliation also in G3 and G14 is reflected in minor N100-N280 peaks in their strike rose diagrams (Fig. 2b) and confirmed by the 3D data (Figs. 7a and 8a).

In view of the above interpreted polyphase evolution, we must now reconsider the significance of predominantly anticlockwise curving inclusion trails in sections striking close to the regional lineation being viewed towards the west. We were not able to determine the ratio's of clockwise vs. anticlockwise ratio's associated with each of the 3 internal foliation sets that have been distinguished. However, it is likely that the curvature sense of inclusion trails in thin sections striking N330, N0, N30 and N60 is mainly determined by the oldest (NE-striking) and youngest (E-W striking) internal sets as these that intersect those thin section planes at a high angle. In contrast, the intermediate NNW-SSE striking inclusion trail set should produce opposite curvature senses in the same thin sections and this might be the reason why about 25% of all garnet porphyroblasts we counted curve in opposite direction as the other 75%.

In summary, the oldest NE-SW striking inclusion trails may be linked to NW directed subduction and SE directed thrusting. The polarity of the intermediate NNW-SSE striking internal foliation remains undetermined. The dominant asymmetry of the youngest WNW-ESE striking trails included in garnet rims of G11 and G12 and in lawsonite are consistent with N-directed subduction.

The reversed curvature sense of inclusion-trails in the pseudomorphs of sample G11 indicates a change to top-to-the-N shearing on the penetrative subhorizontal crenulation cleavage, which caused refolding and transposition all previous fabrics and structures. Shelley and Bossière (2005) related this deformation to wholesale crustal thinning and exhumation. However, considering that HP metamorphism of Ile de Groix rocks is Late-Devonian (360-370Ma; Bosse et al., 2005) and that the Variscan orogeny continued until at least 300Ma, we vertical shortening can also be considered in the context of a gravitationally spreading thrust wedge with plate convergence and subduction continued below the wedge (cf. Bell & Johnson, 1992 - their Figs 16 and 17).

9. Correlation of microstructural- and field data

In this section we review field data from previous workers and assess their relationship with the new microstructural data. Cogné et al (1966) made numerous structural observations and measurements all along the coast of the island and concluded 2 principle deformation

https://doi.org/10.5194/se-2020-175
Preprint. Discussion started: 19 October 2020
© Author(s) 2020. CC BY 4.0 License.

Solid Earth
Discussions
Open Access
EGU

phases, apart from a third post-metamorphic phase that created E-W trending chevron-type folds. Their first deformation was responsible for tight to isoclinal folds with strongly sheared limbs associated with a stretching/mineral lineation. The average trend of these 'fundamental folds' as they called them is N165 in the south east of the island, N-S in the east and changes to NW-SE in the north-west. The second deformation phase caused refolding of the 'fundamental' folds associated with a steeply SW dipping crenulation cleavage trending N130-140. Significantly, Cogné et al. (1966) noticed that mineral lineations defined by glaucophane exhibit highly variable relationships with respect to fold axes, commonly being parallel to them, but locally oblique and clearly predating the folding, or still elsewhere associated with the younger refolding event. I this last case, 2 sets of glaucophane lineations were locally observed oblique to each other (see their Fig. 12, p 70).

Boudier and Nicolas (1976) distinguished 4 deformation phases (D1-D4), the youngest of which corresponds to the chevron-type structures of Cogné et al. (1966). D1 refers to the mineral-lineation (L_1) which they interpreted to have been reoriented by N165 trending folds (D2 and D3). At an outcrop studied in particular detail at Vallon du Lavoir (Fig. 2a), a N120 orientation maximum of L_1 was found (Fig. 9b) and interpreted as the original trend. This opposes Cogné et al.'s (1966) interpretation of early N165 trending folds overprinted by younger N130 ones, which is in better agreement with our microstructural data. An unpublished sketch and corresponding orientation measurements by Claude Audren (1974; redrafted in Fig. 9a), held at the 'Maison de la Reserve Naturelle Le Bail' on Ile de Groix, further supports Cogné et al.'s (1966) and our interpretation by depicting refolding of a N165 lineation around a N120 trending fold axes.

Quinquis & Choukroune (1980) endorsed a late origin of the N120 trending folds described by Cogné et al. (1966) but considered them post-metamorphic structures. In their view, the N120 maximum defined by glaucophane at Vallon du Lavoir is only coincidental and without regional tectonic significance. They predicted that on a regional scale the lineation varies symmetrically between N120 and N200 due to sheath folding driven by top-to-N340 progressive shearing. However, their interpretation was based principally on analogue modeling of sheath folds (Cobbold & Quinquis, 1980) rather than on new structural or microstructural data.

The above contradictory interpretations of the original orientation of L1 and its timing relative to folding are not surprising in view of the polyphase character of 'L1' associated with different foliations shown herein and recognized earlier by Cogné et al. (1966). Significantly, the bimodal trends of L1 seen in the field data Boudier & Nicolas (1976) collected across the

https://doi.org/10.5194/se-2020-175
Preprint. Discussion started: 19 October 2020
© Author(s) 2020. CC BY 4.0 License.

Solid Earth Discussions

island (Fig. 9c, 10a) reflect the orientations of the 3 sets of inclusion trails distinguished in this paper.

10. Pouldu schists, Tréogat Formation and Central Armorican Domain samples

The 'Pouldu schists' are greenschists of volcano-sedimentary origin (Triboulet, 1992) locally hosting abundant plagioclase porphyroblasts. Inclusion trails in these crystals were measured in 3 oriented samples (PO2, Po3, PO5) plus a fourth sample (AU-1) collected from a similar greenschist unit known as the Tréogat Formation (Luck et al., 2002) cropping out in the Baye d'Audièrne. Inclusion trails in these samples broadly strike E-W and are tentatively correlated with the also E-W to WNW-ESE striking youngest internal foliation found in garnets and lawsonite of Ile de Groix. Three of these samples contain a N060 striking crenulation cleavage in the matrix, which is included in the rims of some porphyroblasts.

(NOTE TO EDITOR AND REVIEWERS: we have not received on time 4 N-S striking vertical thin sections of these samples, in which we plan to determine the curvature sense of inclusion trails. We hope to incorporate that extra data in a later version of this manuscript).

Two staurolite-kyanite schists from the Central Armorican Domain, located about 5km NNE of Quimper, were also studied. The age of metamorphism in these 2 samples is roughly constrained by granite ages to the period of 350-320Ma (Schulz et al., 1998), and hence post-dates the high-pressure metamorphism (360-370Ma) of Ile de Groix. Inclusion trails in these samples trend N060 and my correlate with the N060 crenulation cleavage observed in the matrix of our greenschist samples.

11. Discussion

11.1. Comparison with inclusion-trails in NW-Iberia

Figure 10 compares our new inclusion-trail data from Brittany are compared with that of Aerden (2004) for the Basal Unit of the allochthonous complexes of NW-Iberia. This unit comprises orthogneises and high-pressure micaschists retrogressed in greenschist facies representing the subducted margin of Gondwana (Arenas et al, 1995; Martínez-Catalán, 1996) with a similar structural position as the Pouldu Schists, below an ophiolitic unit. Three sets of inclusion trails striking E-W, NE-SW and NNW-SSE were distinguished in this unit preserved in plagioclase and garnet porphyroblasts. The oldest of these with E-W trend were

https://doi.org/10.5194/se-2020-175
Preprint. Discussion started: 19 October 2020
© Author(s) 2020. CC BY 4.0 License.

471 related to the high-pressure event dated 370-360Ma (Van Calsteren et al., 1979; Santos
472 Zalduegui, et al. 1995; Abati et al., 2010; Li & Massonne, 2017), and hence synchronous with
473 the metamorphism of Ile de Groix (Bosse et al., 2005). The 2 younger internal foliations sets
474 formed at lower pressures and their age was only loosely constrained to pre-320 Ma.
475 To account for the Cretaceous anticlockwise rotation of Iberia during formation of the
476 Gulf of Biscay, the current northern margin Iberian is placed back against the conjugate
477 margin of south Brittany in Fig. 10 implying 20° clockwise back-rotation of Iberia. Although
478 this reconstruction produces a good match of inclusion-trail strikes in both massifs (Fig. 10b),
479 it poses question around the relative timing evidence of Aerden (2004). He interpreted that the
480 (presently) NNW-SSE striking inclusion trails in the Basal Unit (colored blue in Fig. 9)
481 postdate E-W striking ones (yellow), opposite to what has been concluded herein. As he
482 based this on only a sample with bimodal strikes of inclusion trails (sample 1. - Fig. 9a) we
483 believe there is scope for re-assessing the relative timing of Aerden (2004) using X-ray
484 tomography.
485 In contrast, the relative timing of NW-SE striking inclusion trails in NW Iberia
486 (marked with red lines in Fig. 9) was based on more abundant microstructural and field
487 criteria. Consequently, these microstructures cannot be correlated with much older NW-SE
488 trails in samples of Ile de Groix, but a correlation is possible with internal foliations in the 2
489 samples from the Central Armorican Domain, and the crenulation cleavages in the Pouldu
490 schists (Fig. 2c and d).
491 We checked the curvature sense of inclusion trails in Aerden's (2004) thin sections
492 associated with the W-E to NW-SE FIAs (marked yellow in Fig. 10a) this author determined
493 in 6 samples of the Basal-Unit. In samples 3-4, 10, 14 and 20, inclusion trails curve
494 anticlockwise viewing west. In samples 2 and 19 they curve clockwise. A larger number of
495 anticlockwise trails is as observed in Ile de Groix, but we realize that more samples need to be
496 studied before firm conclusions can be drawn regarding thrusting directions in NW Iberia.
497
498 *11.2. Origin of sheath folds*
499
500 Based on a study of quartz fabrics in 57 samples, Shelley and Bossière (1999)
501 concluded that many of the folds of Ile de Groix island nucleated with their axes subparallel
502 to the maximum stretching direction (X) instead of parallel to Y and subsequently rotating
503 towards X by progressive shearing (cf. Quinquis and Choukroune, 1981). Both models
504 assume a single progressive deformation with subhorizontal flow plane that ignores the

https://doi.org/10.5194/se-2020-175
Preprint. Discussion started: 19 October 2020
© Author(s) 2020. CC BY 4.0 License.

Solid Earth
Discussions
Open Access
EGU

505 polyphase character of the main foliation and lineation shown herein. This complexity places
506 the significance of fold-axes parallel stretching lineations and the origin of non-cylindrical
507 folds in a quite different light. We interpret these as having formed by vertical flattening
508 superposed on folds with steeply dipping axial planes and variably plunging fold-axes (Fig.
509 10). Depending on the original geometry of precursor folds, new folds nucleated with straight
510 axes parallel to X or with strong curvature.
511
512 **12. Conclusion**
513
514 (1) The blueschist-eclogite facies rocks of Ile de Groix experienced 4 successive
515 tectonic events potentially reflected in a also complex PT path (Schulz et al., 2001).
516 Corresponding fabrics are preserved as inclusion trails that maintained their original
517 orientations due to limited or no rotation of porphyroblasts during ductile deformation.
518 (2) In specific orientations and dominant curvature sense of inclusion trails allow the
519 following reconstruction. (Stage-I) Early NW-directed subduction of Gondwana. (Stage-2) E-
520 W crustal shortening with unconstrained subduction polarity, but probably to westward given
521 the preceding subduction direction. (Stage III) Northward subduction until peak metamorphic
522 conditions were reached. (Stage IV) Exhumation associated with vertical shortening and a
523 component of top-to-the-north shearing indicated by the asymmetry of inclusion trails in
524 lawsonite pseudomorphs as well as late shear bands (Philippon et al, 2009). A subhorizontal
525 crenulation cleavage associated with this event transposes all earlier fabrics. Inclusion-trails
526 studied in 4 additional greenschist samples from the lower-grade footwall of the Groix
527 ophiolite strike E-W, parallel to the youngest set of inclusion trails in the blueschist samples
528 from the island.
529 (3) The curvature sense of sigmoidal and spiral-shaped inclusion trails indicates top-
530 to-the south thrusting which agrees with regional-geological evidence only when a 'non-
531 rotational' original of these microstructures is accepted. The traditional 'rotational'
532 interpretation implied an opposite and shear sense conflicting with the regional tectono-
533 metamorphic structure of southern Brittany.
534 (4) The strikes of 3 sets of inclusion trails documented herein can be tentatively
535 correlated with 3 similar sets reported earlier in NW-Iberia (Aerden, 2004). The coincidence
536 of microstructural directions between both regions is maximized assuming only 20° rotation
537 of Iberia during opening if the Gulf of Biscay, significantly less as ca. 35° rotation generally
538 concluded from paleomagnetic data (Gong et al., 2009).

https://doi.org/10.5194/se-2020-175
Preprint. Discussion started: 19 October 2020
© Author(s) 2020. CC BY 4.0 License.

Solid Earth
Discussions
Open Access
EGU

(5) Fold axes parallel to stretching lineations and rare sheath folds reported on Groix did not form by progressive uni-direction shearing, but by vertical shortening and horizontal shearing superposed on steeply dipping pre-existing foliations and folds with variable plunges.

Acknowledgements

The first author wishes to thank José Ramón Martínez Catalán for his support and friendship ever since he started a postdoc in Salamanca in 1996. We thank Michel Ballèvre for helping us obtain permission to collect samples on Ile de Groix and for suggesting we sample the Pouldu schists as well. Ile de Groix national-park guide Catherine Robert (and her dog) provided Aerden with helpful information and pleasant company during field work. Bernhardt Schulz is thanked for clarifying various aspects about the petrology of the studied rocks. This research was partially funded by a travel grant from Junta de Andalucía to Aerden in 2006. ...Reviewers, Editors.....

References

Aerden, D.G.A.M., (1995) Porphyroblast non-rotation during crustal extension in the Variscan Pyrenees. Journal of Structural Geology 17, 709-726.

Aerden, D.G.A.M., (1998) Tectonic evolution of the Montagne Noire and a possible orogenic model for syn-collisional exhumation of deep rocks, Hercynian belt, France. Tectonics 17, 62-79.

Aerden, D.G.A.M., (2004) Correlating deformations in the Iberian Massif (Variscan belt) using porphyroblasts; implications for the development of the Ibero-Armorican Arc. Journal of Structural Geology 26, 177-196.

Aerden, D.G.A.M., Bell, T.H., Puga, E., Sayab, M., Lozano, J.A., Díaz de Federico, A., (2013) Multi-stage mountain building vs. Relative plate motions in the Betic Cordillera deduced from integrated microstructural and petrological analysis of porphyroblast inclusion trails. Tectonophysics 587, 188-206.

Aerden, D.G.A.M., Ruiz-Fuentes, A., (2020) X-ray computed microtomography of spiral garnets: A new test of how they form. Journal of Structural Geology 136. https://doi.org/10.1016/j.jsg.2020.104054

Arenas, R., Rubio Pascual, F., Díaz García, F., Martínez Catalán, J.R., (1995) High-pressure micro-inclusions and development of an inverted metamorphic gradient in the Santiago

https://doi.org/10.5194/se-2020-175
Preprint. Discussion started: 19 October 2020
© Author(s) 2020. CC BY 4.0 License.

573 Schists (Ordenes Complex, NW Iberian Massif, Spain): evidence of subduction and
574 syncollisional decompression. Journal of Metamorphic Geology 13, 141–164.
575 Arenas, R., Sanchez Martinez, S., Diez Fernandez, R., Gerdes, A., Abati, J., Fernandez-
576 Suarez, J., Andonaegui, P., Cuadra, P.G., Carmona, A.L., Albert, R., Fuenlabrada, J.M.,
577 Rubio Pascual, F.J., (2016) Allochthonous terranes involved in the Variscan suture of NW
578 Iberia: A review of their origin and tectonothermal evolution Earth-Science Reviews 161,
579 140-178.
580 Azor, A., Rubatto, D., Simancas, J.F., González Lodeiro, F., Martínez Poyatos, D.,
581 MartínParra, L.M., Matas, J., (2008) Rheic Ocean ophiolitic remnants in southern Iberia
582 questioned by SHRIMP U–Pb zircon ages on the Beja-Acebuches amphibolites. Tectonics
583 27, TC5006.
584 Ballevre, M; Pitra, P; Bohn, M., (2003) Lawsonite growth in the epidote blueschists from the
585 Ile de Groix (Armorican Massif, France): a potential geobarometer. Journal of
586 Metamorphic Geology 21, 723-735.
587 Ballèvre, M., Bosse V., Ducassou, C., Pitra. P., (2009) Palaeozoic history of the Armorican
588 Massif: Models for the tectonic evolution of the suture zones. C. R. Geoscience 341 (2009)
589 174–201.
590 Ballevre, M., Bosse, V., Dabard, M.P., Ducassou, C., Fourcade, S. et al., (2015) Histoire
591 Géeologique du massif Armoricain : Actualitée de la recherche. Bulletin de la Sociétée
592 Géologique et Minéralogique de Bretagne, Société géologique et minéralogique de
593 Bretagne, (2013, (D), 10-11, pp.5-96. <insu-00873116>
594 Bell, T.H., (1985) Deformation partitioning and porphyroblast rotation in metamorphic rocks:
595 A radical reinterpretation. Journal of Metamorphic Geology 3, 109-118.
596 Bell. T. H., Rubenach, M. J. & Flemming, P. D., (1986) Porphyroblast nucleation, growth and
597 dissolution in regional metamorphic rocks as a function of deformation partitioning during
598 foliation development. Journal of Metamorphic Geology, 4, 37–67.
599 Bell, T.H, Sapkota, J., (2012) Episodic gravitational collapse and migration of the mountain
600 chain during orogenic roll-on in the Himalayas. Journal of Metamorphic Geology 30, 651-
601 666.
602 Bell, T. H., & Sanislav, I. V., (2011) A deformation partitioning approach to resolving the
603 sequence of fold events and the orientations in which they formed across multiply
604 deformed large-scale regions. Journal of Structural Geology, 33(7), 1206–1217.
605 https://doi.org/10.1016/j.jsg.2011.03.014

https://doi.org/10.5194/se-2020-175
Preprint. Discussion started: 19 October 2020
© Author(s) 2020. CC BY 4.0 License.

606 Bell, T.H., Forde, A., Wang, J., (1995) A new indicator of movement direction during
607 orogenesis - measurement technique and application to the Alps. Terra Nova 7, 500-508.
608 Bell, T.H., Hickey, K.A., Upton, G.J.G., (1998) Distinguishing and correlating multiple
609 phases of metamorphism accross a multiply deformed region using the axes of spiral,
610 staircase, and sigmoidally curved inclusion trails in garnet. Journal of Metamorphic
611 Geology 16, 767-794.
612 Bell, T.H., Johnson, S.E., Davis, B., Forde, A., Hayward, N., Wilkins, C., (1992)
613 Porphyroblast inclusion-trail orientation data: eppure non son girate! Journal of
614 Metamorphic Geology 10, 295-307.
615 Bosse V., Ballèvre M., Vidal O., (2002) Ductile thrusting recorded by the garnet isograd from
616 blueschist-facies metapelites of the Île de Groix, Armorican Massif, France. Journal of
617 Petrology 43, 485-510.
618 Bosse, V., Féraud, G., Ballèvrec, M., Peucatc, J.J., Corsini, M., (2005) Rb–Sr and 40Ar/39Ar
619 ages in blueschists from the Ile de Groix (Armorican Massif, France): Implications for
620 closure mechanisms in isotopic systems. Chemical Geology 220 (2005) 21– 45.
621 Cannat, M., (1985) Quartz microstructures and fabrics in the island of Groix (Brittany,
622 France). Journal of Structural Geology 7, 555–562
623 Cobbold, P.R., Quinquis, H., (1980) Development of sheath folds in shear regimes. Journal of
624 Structural Geology 2, 119-126.
625 Cogné J., Daniel, J., Ruhland, M., (1966) L'Ile de Groix. Etude structurale d'une série
626 métamorphique à glaucophane en Bretagne méridionale. In: Bulletin du Service de la carte
627 géologique d'Alsace et de Lorraine, 19-1, pp. 41-96. doi :
628 https://doi.org/10.3406/sgeol.1966.1298
629 Díaz García, F., Arenas, R., Martínez Catalán, J.R., González del Tánago, J., and Dunning,
630 G.R., (1999) Tectonic evolution of the Careón ophiolite (northwest Spain): A remnant of
631 the oceanic lithosphere in the Variscan Belt. Journal of Geology, v. 107, p. 587–605.
632 Doube M, Kłosowski MM, Arganda-Carreras I, Cordeliéres F, Dougherty RP, Jackson J,
633 Schmid B, Hutchinson JR, Shefelbine SJ. (2010) BoneJ: free and extensible bone image
634 analysis in ImageJ. Bone 47:1076-9. doi: 10.1016/j.bone.2010.08.023
635 Faure, M., Bé Mézème, E., Cocherie, A., Rossi, P., Chemenda, A., Boutelier, D., (2008)
636 Devonian geodynamic evolution of the Variscan Belt, insights from the French Massif
637 Central and Massif Armoricain, Tectonics, 27, TC2005, doi:10.1029/2007TC002115.

https://doi.org/10.5194/se-2020-175
Preprint. Discussion started: 19 October 2020
© Author(s) 2020. CC BY 4.0 License.

638 Felix, C., Fransolet, A.M., (1972) Pseudomorphes á épidote s.l., paragonite, muscovite s.l.,
639 chlorite, albite. de porphyroblastes de lawsonite (?) dans les glaucophanites de l'Île de
640 groix (bretagne – France). Annales de la Société Geologique de Belgique 95, 323–334.
641 Gong, Z., Langereis, C.G., Mullender, T.A.T. , (2008) The rotation of Iberia during the
642 Aptian and the opening of the Bay of Biscay. Earth and Planetary Science Letters 273, 80–
643 93.
644 Hayward, N., (1990) Determination of early fold axis orientations in multiply deformed rocks
645 using porphyroblast inclusion trails. Tectonophysics 179, 353-369.
646 Hayward, N., (1992) Microstructural analysis of the classical spiral garnet porphyroblasts of
647 south-east Vermont: evidence for non-rotation. Journal of Metamorphic Geology 10, 567-
648 587.
649 Huddlestone-Holmes, C.R., Ketcham, R.A., (2005) Getting the inside story: using computed
650 X-ray tomography to study inclusion trails in garnet porphyroblasts. American
651 Mineralogist 90. DOI: 10.2138/am.2005.1840.
652 Huddlestone-Holmes, C.R., Ketcham, R.A., (2010) An X-ray computed tomography study of
653 inclusion trail orientations in multiple porphyroblasts from a single sample.
654 Tectonophysics 480, 305–320.
655 Kim, H.S., Sanislav, I.V. (2017). Foliation intersection/inflection axes within porphyroblasts
656 (FIAs): a review of advanced applications and significance. Geosciences Journal 21,
657 1013-1032. http://dx.doi.org/10.1007/s12303-017-0047-z
658 Lagarde, J.L. (1980). La déformation des roches dans les domaines àschistosité
659 subhorizontale. Applications à la nappe du Canigou-Roc de France (Pyrénées orientales) et
660 au complexe crystallophyllien de Champtoceaux (Massif armoricain). Unpublsihed PhD
661 thesis, Université de Rennes, 170 p.
662 Li, B., Massonne, H.J., (2017) Contrasting metamorphic evolution of metapelites from the
663 Malpica-Tuy unit and the underlying so-called parautochthon at the coast of NW Spain.
664 Lithos 286–287, 92–108. http://dx.doi.org/10.1016/j.lithos.2017.06.003
665 Mares, V.M., (1998) Structural development of the Soldiers Cap Group in the Eastern Fold
666 Belt of the Mt Isa Inlier: a successive of horizontal and vertical deformation events and
667 large-scale shearing. Aust. J. Earth Sci. 45, 373–387.
668 Martínez Catalaín, J.R., Arenas, R., Díaz García, F., Rubio Pascual, F.J., Abati, J., Marquínez,
669 J., (1996) Variscan exhumation of a subducted Palaeozoic continental margin: the basal
670 units of the Ordenes Complex, Galicia, NW Spain. Tectonics 15, 106–121.

https://doi.org/10.5194/se-2020-175
Preprint. Discussion started: 19 October 2020
© Author(s) 2020. CC BY 4.0 License.

671 Martínez-Catalán, J.R., (2012) The Central Iberian arc, an orocline centered in the Iberian
672 Massif and some implications for the Variscan belt. Int J Earth Sci (Geol Rundsch)
673 101:1299–1314. DOI 10.1007/s00531-011-0715-6
674 Munro, M. A., & Blenkinsop, T. G. (2012). MARD - A moving average rose diagram
675 application for the geosciences. Computers & Geosciences, 49, 112–120.
676 https://doi.org/10.1016/j.cageo.2012.07.012
677 Philippon M., Brun J.-P. et Gueydan F., (2009) Kinematic records of subduction and
678 exhumation in the Île de Groix blueschists (Hercynian belt ; Western France). Journal of
679 Structural Geology 31, 1308-1321.
680 Quinquis, H., Audren, C., Brun, J. P. & Cobbold, P. R. (1978) Intense shear in Ile de Groix
681 blueschists and compatibility with subduction or obduction. Nature, Lond. 273, 43-45.
682 Quinquis, H., (1980) Schistes bleus et déformation progressive: l'exemple de l'Île de Groix
683 (Massif Armoricain). Université de Rennes 1.
684 Quinquis, H., Choukroune, P., (1981) The Ile de Groix blueschists in the Hercynian chain -
685 kinematical implications. Bulletin de la societe geologique de France 2, 409-418.
686 Rosenfeld, J.L., (1970) Rotated garnets in metamorphic rocks. Geological Society of America
687 Special Paper 129, 102pp.
688 Sayab, M., (2005) Microstructural evidence for N–S shortening in the Mount Isa Inlier (NW
689 Queensland, Australia): the preservation of early W–E-trending foliations in
690 porphyroblasts revealed by independent 3D measurement techniques. Journal of Structural
691 Geology 27, 1445-1468.
692 Shah, S.Z. Sayab, M., Aerden, D.G.A.M, Asif-Kahn, M. (2011) Foliation intersection axes
693 preserved in garnet porphyroblasts from the Swat area, NW Himalaya: A record of
694 successive crustal shortening directions between the Indian plate and Kohistan-Ladakh
695 Island Arc. Tectonophysics 509, 14-32.
696 Shelley, D., Bossieère, G., (1999) Ile de groix: retrogression and structural developments in
697 an extensional régime. Journal of Structural Geology 21, 1441–1455.
698 Schindelin, J., Arganda-Carreras, I., Frise, E., Kaynig, V., Longair, M., Pietzsch, T., Preibisch,
699 S., Rueden, C., Saalfeld, S., Schmid, B., Tinevez, J.Y., White, D.J., Hartenstein, V.,
700 Eliceiri, K., Tomancak, P., Cardona, A., (2012) Fiji: an open-source platform for
701 biological-image analysis. Nature Methods 9, 676-682.
702 Schulz, B., Triboulet., C., Audren., C; Pfeifer., H.R., Gilg, A., (2001) Two-stage prograde and
703 retrograde Variscan metamorphism of glaucophane-eclogites, blueschists and greenschists
704 from Ile de Groix (Brittany, France) International Journal of Earth Sciences, 90, 871-889.

https://doi.org/10.5194/se-2020-175
Preprint. Discussion started: 19 October 2020
© Author(s) 2020. CC BY 4.0 License.

Spry, A., 1633) The origin and sigdicance of snowball structure in garnet. Journal of Petrology 4, 211-222.

Stallard, A.R., Hickey, K.A., Upton, G.J., (2003) Measurement and correlation of microstructures: the case of foliation intersection axes. Journal of Metamorphic Geology 21, 241–252.

Triboulet, C., (1974) Les glaucophanites et roches associe´es de l'île de Groix (Morbihan, France): étude minéralogique et pétrogénétique. Contributions to Mineralogy and Petrology, 45, 65–90.

Zwart, H., (1962) On the determination of polymorphic mineral associations and its application to the Bosost area (central Pyrenees). Geologisches Rundschau, 52, 38-65.

FIGURE CAPTION

Fig. 1. Simplified geological maps of southern Brittany and NW-Iberia showing the location of ophiolite outcrops and samples studied herein and by Aerden (2004) in NW Iberia.

Fig. 2. (a) Stretching lineation pattern of Ile de Groix and sample locations. (b) Moving-average rose diagrams for inclusion-trail strikes. Encircled pie-cake symbols represent average FIA trends in samples determined from radial thin sections and the FIA plunge direction. Also the sense of inclusion-trail curvature is indicated viewing down the FIA plunge (anticlockwise in G14, G12, G11; clockwise in G19 and G7). (c) Data for samples from the Pouldu schistes (PO2, 3, 5) and the Tréogat formation (AU1). Arrows represent crenulation axes in the matrix. (d) Data for 2 staurolite-kyanite schists from the Central Armorican Domain. The 4 inclusion-trail sets proposed in this paper are marked with magenta, blue, yellow and red trend lines, from the oldest to the youngest set.

Fig. 3. (a) Rotational interpretation of sigmoidal and spiral-shaped inclusion trails from Ile de Groix and the range (purple) of inclusion trail strikes predicted by this model. (b) 'Non-rotational' interpretation of the same inclusion trails according to Bell et al (1986) and Bell & Johnson (1989) consistent with orthogonal truncations and inclusion trails striking subparallel to stretching lineations, crenulation- and fold-axes. (c) Strikes measured in all 10 samples from Groix agree better with the non-rotational model.

https://doi.org/10.5194/se-2020-175
Preprint. Discussion started: 19 October 2020
© Author(s) 2020. CC BY 4.0 License.

739 Fig. 4. (a) Sketches of well developed 'rotational' inclusion trails in oriented vertical thin
740 sections of samples G7 and G14 showing vertical and horizontal alignment of internal
741 truncations (purple lines). (b) Rose diagram plotting the orientations of all individual dashes
742 that make up the dashed lines representing inclusion trails in the drawings measured with the
743 image/analysis program *Fiji*. The plot demonstrates bimodal orientations of the inclusion
744 trails related to the orthogonal sets of truncations.
745
746 Fig. 5. All photographs of G11. (a and b) Garnet porphyroblast (parallel and crossed polars)
747 with sigmoidal trails in a N-S striking vertical section. Barb of N-arrow points upward. Note
748 top-to-the south shear sense suggested by asymmetric strain shadows, inconsistent with
749 porphyroblast rotation. (c) Garnet with spiral-shaped truncation inclusion trails a
750 porphyroblast core and rim zone. (d) Opaque mineral with elongate shape replaced by
751 Goethite. (e and f). Lawsonite pseudomorphs (parallel and crossed polars) showing weakly
752 sigmoidal inclusion trails oblique to the matrix foliation. (g) Tomographic image of a strongly
753 curved inclusion trails garnet in G12. (h) Tomographic image of an elongate lawsonite
754 pseudomorph, garnet (Gt) and opaque large opaque crystal.
755
756 Fig. 6. Stereoplots (equal angle, lower hemisphere) of internal foliations and FIAs measured
757 in garnet and lawsonite pseudomorphs in samples G11 and G12. Also shown are 2 contoured
758 stereoplots plotting maximum and minimum elongation directions of relatively large opaques
759 present in the matrix of G11 and G12. See legend. The data can be matched to different sets
760 of inclusion trails drawn with corresponding colors in garnets and a representative lawsonite
761 pseudomorphs. The Mn concentration map is for one of the porphyroblasts with truncational
762 inclusion trails.
763
764 Fig. 7. Tomographic images and microstructural data for sample G14. (a) Stereoplot of
765 internal foliation planes, FIAs (grey boxes), long- and short axes of opaque minerals, and the
766 axial plane of cm-scale folds. (b and c) Map- and cross-section views of a fold outlined by an
767 epidote-rich layer. Its axial trace trends NNE-SSW oblique to N-S trending cross-cutting
768 cleavage zones also visible in (d). The cross-section shows refolding with subhorizontal axial
769 planes suggesting a component of vertical flattening associated with the main cleavage
770 (compare with Fig. 4a, b).
771

https://doi.org/10.5194/se-2020-175
Preprint. Discussion started: 19 October 2020
© Author(s) 2020. CC BY 4.0 License.

Solid Earth
Discussions
Open Access
EGU

772 Fig. 8. (a) 3D microstructural data for sample G3. See legend for explanation. (b) Field data
773 collected by Claude Audren about 1 km north of at the location of sample G7 (Plage du
774 Trech) and the average FIA trend we determined for this sample from radial thin sections
775 (magenta pie-cake segment). The FIA trend coincides with fold axes measured in the field.
776 Note that this conflicts with models assuming sheath folding and porphyroblast rotation.
777 Stretching lineations vary greatly reflecting the polyphase origin of this fabric.
778
779 Fig. 9. (a) Structural data collected by C. Audren and a corresponding sketch of isoclinal folds
780 he drew at Vallon de Kérigant (location marked in Fig. 2a). The sketch is accurately redrafted
781 and data re-plotted in lower hemisphere, equal angle projection (Audren used upper
782 hemisphere, equal angle). Refolding of a N165 trending lineation around the nose of a N120
783 trending fold is demonstrated. (b) Lineations (L1) measured nearby (a) by Boudier & Nicolas
784 (1976) at Vallon du Lavoir showing a N120 trend maximum of L1 (yellow lines) oblique to
785 B2 fold axes in the same outcrop (blue lines). (c) Structural data from the same authors for the
786 entire island. Note the bimodal pattern of L1. Magenta, blue and yellow trend lines show how
787 this data can be correlated with the 3 sets of inclusion trails given the same colors in Figs 2, 5,
788 7 and 8.
789
790 Fig. 10. (a) Inclusion trails-strikes in the newly studied rocks and those measured by Aerden
791 (2004) in 18 samples form the Basal Unit of NW-Iberia. The microstructures are correlated as
792 4 age sets marked with magenta, blue, yellow and red trend bars (from older to younger sets).
793 Field data from Boudier and Nicolas (1976) and that of Engels (1972) and van Zuuren (1969)
794 also show a good match. (b) Rose diagrams plotting inclusion-trail directions marked blue
795 and yellow for different amounts of Iberia back-rotation. The directions line up best with 20°
796 back-rotation, which is the current angle between the North-Iberia margin and that of southern
797 Brittany.
798
799 Fig. 11. Conceptual models showing how vertical shortening and horizontal stretching can
800 produce highly variable fold geometries depending on the original orientations of folded
801 planes or pre-existing folds. Note how strongly curved fold axes can form without need of
802 extremely large shears trains. Adding a (horizontal) shearing component in the direction of X
803 and/or Y can be expected to further modify the fold-interference patterns.tt

https://doi.org/10.5194/se-2020-175
Preprint. Discussion started: 19 October 2020
© Author(s) 2020. CC BY 4.0 License.

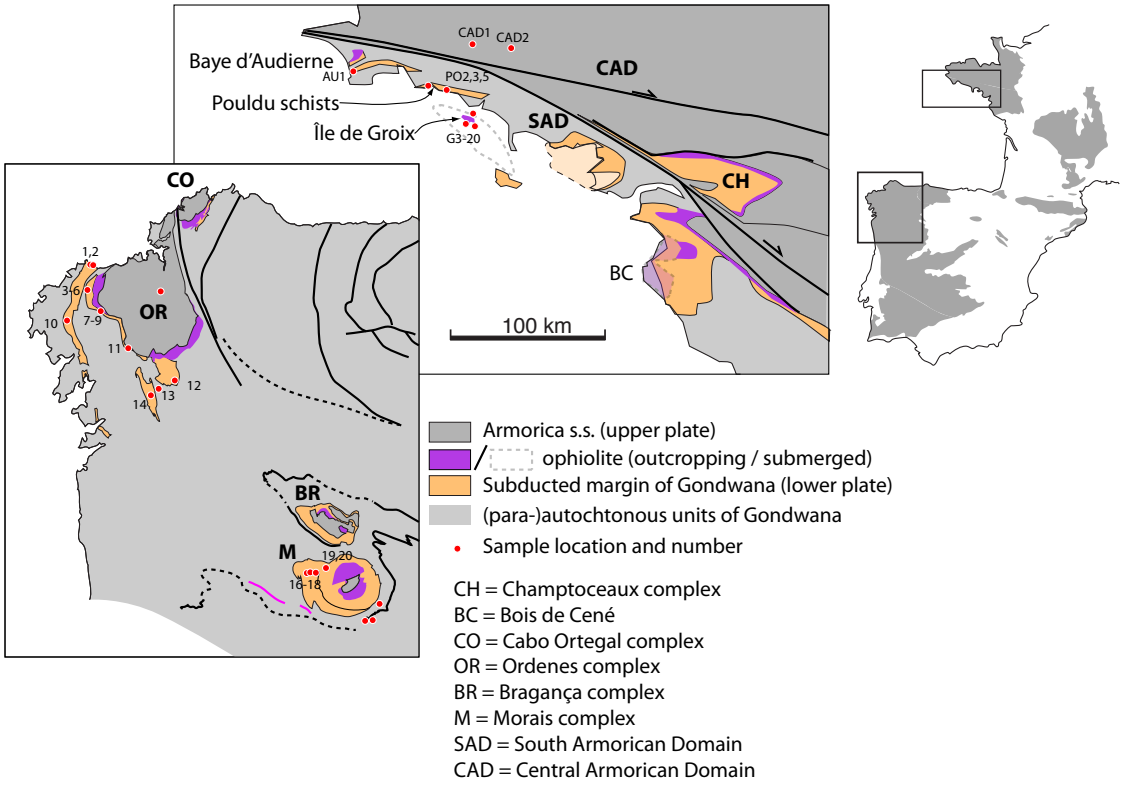

FIG. 1

https://doi.org/10.5194/se-2020-175
Preprint. Discussion started: 19 October 2020
© Author(s) 2020. CC BY 4.0 License.

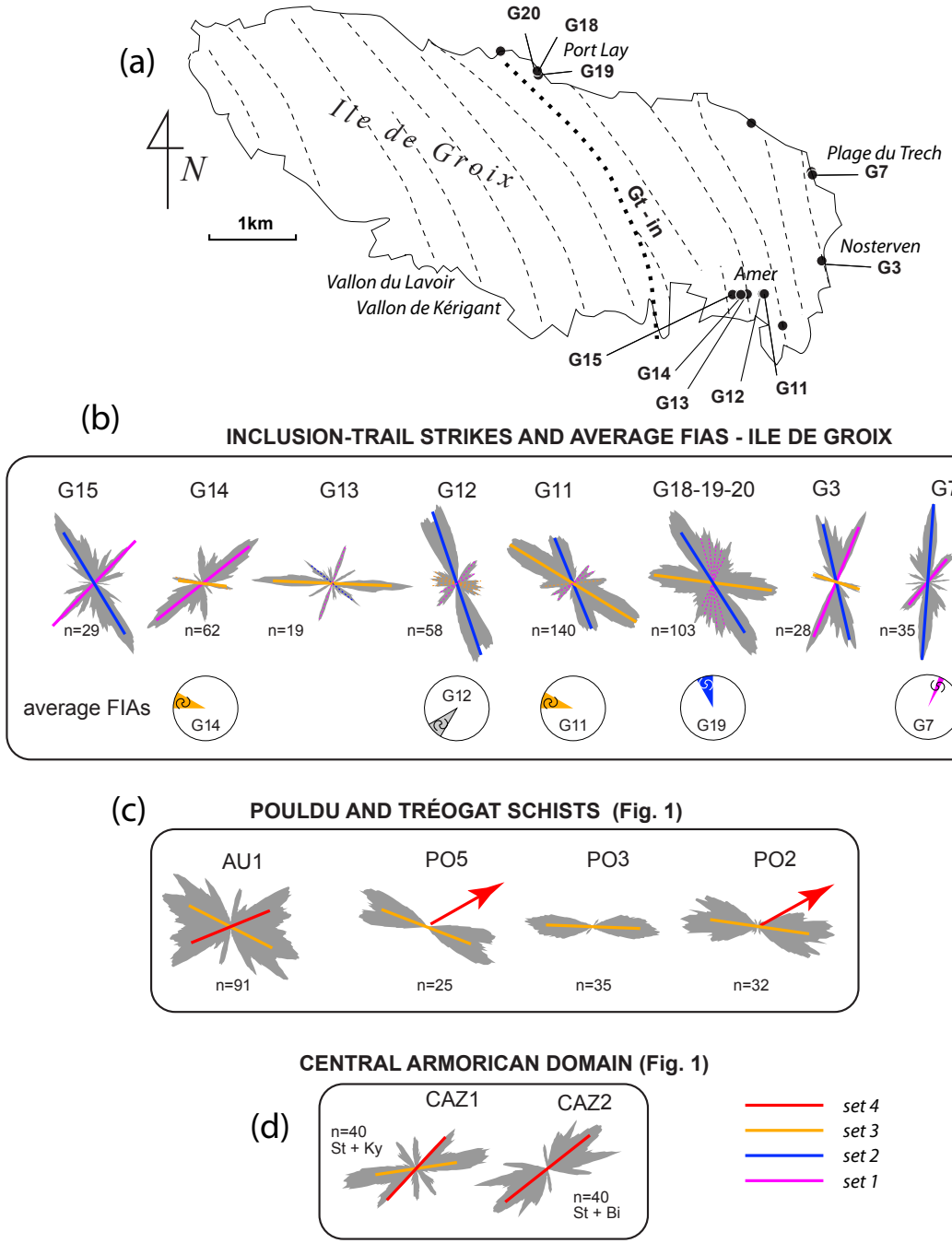

FIG. 2

https://doi.org/10.5194/se-2020-175
Preprint. Discussion started: 19 October 2020
© Author(s) 2020. CC BY 4.0 License.

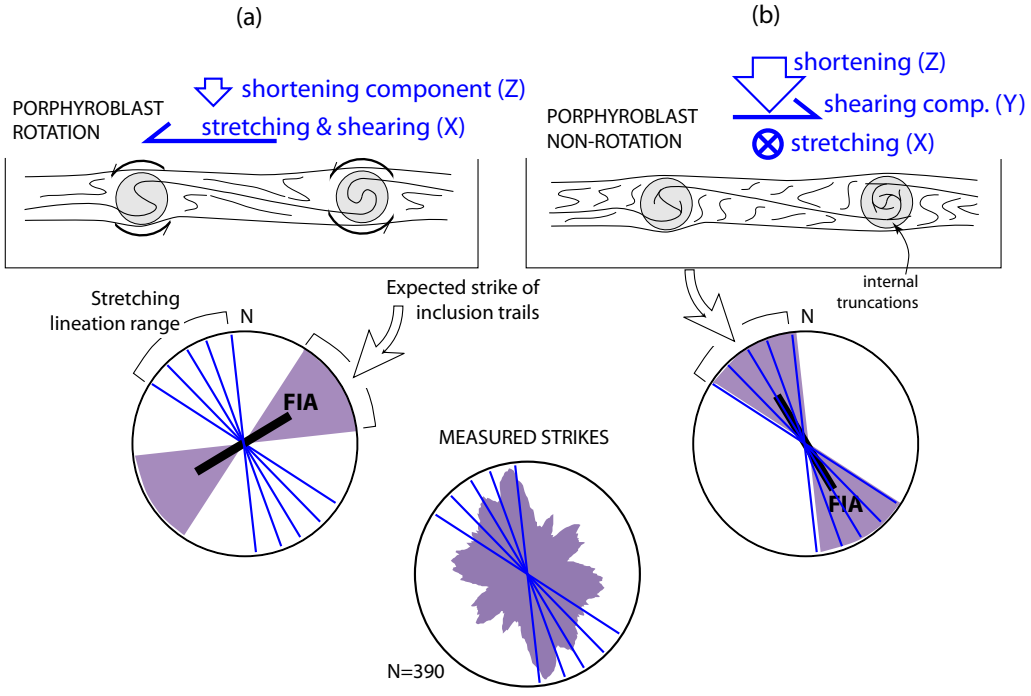

FIG. 3

https://doi.org/10.5194/se-2020-175
Preprint. Discussion started: 19 October 2020
© Author(s) 2020. CC BY 4.0 License.

Solid Earth
Discussions
Open Access
EGU

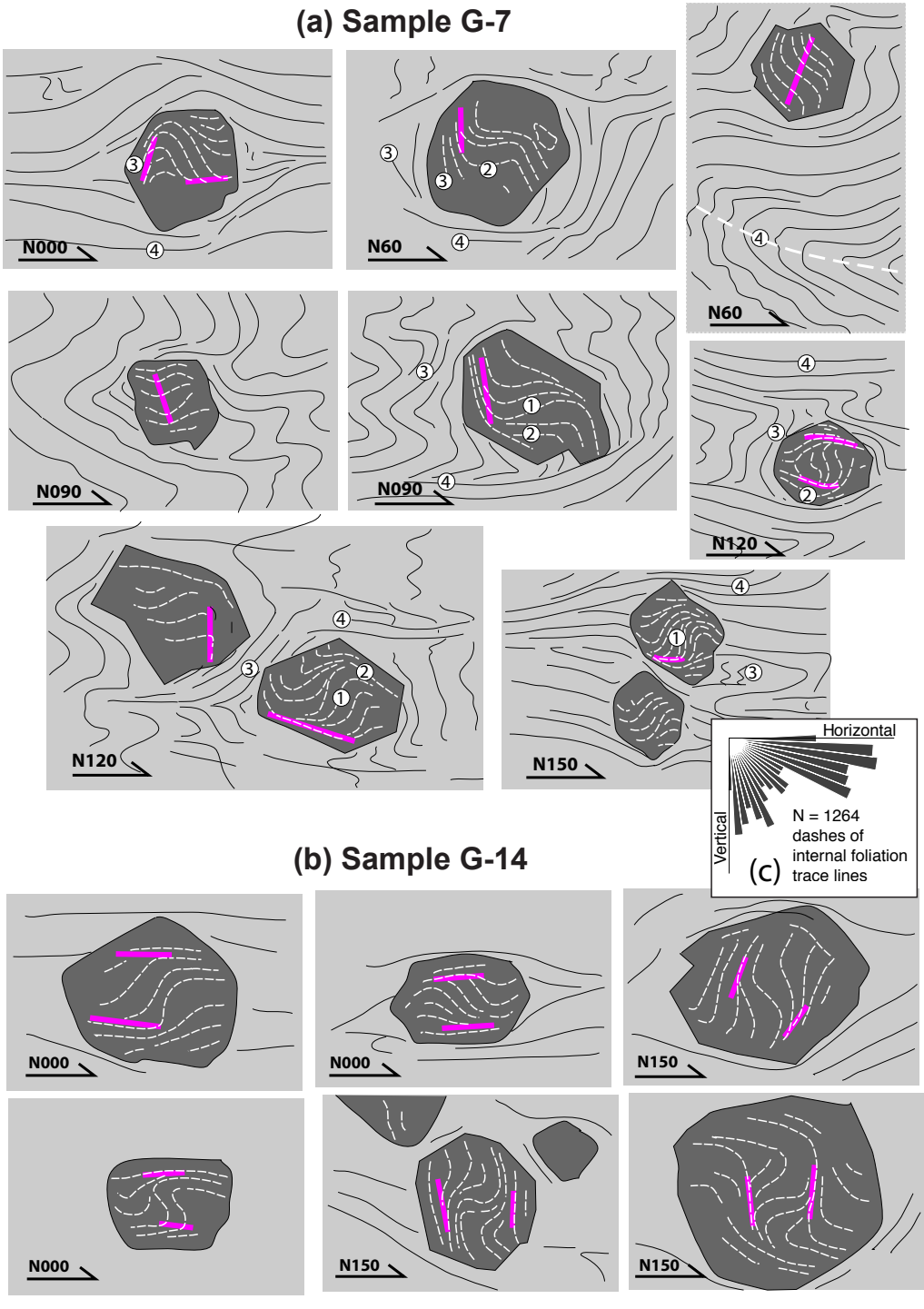

https://doi.org/10.5194/se-2020-175
Preprint. Discussion started: 19 October 2020
© Author(s) 2020. CC BY 4.0 License.

Solid Earth
Discussions
Open Access
EGU

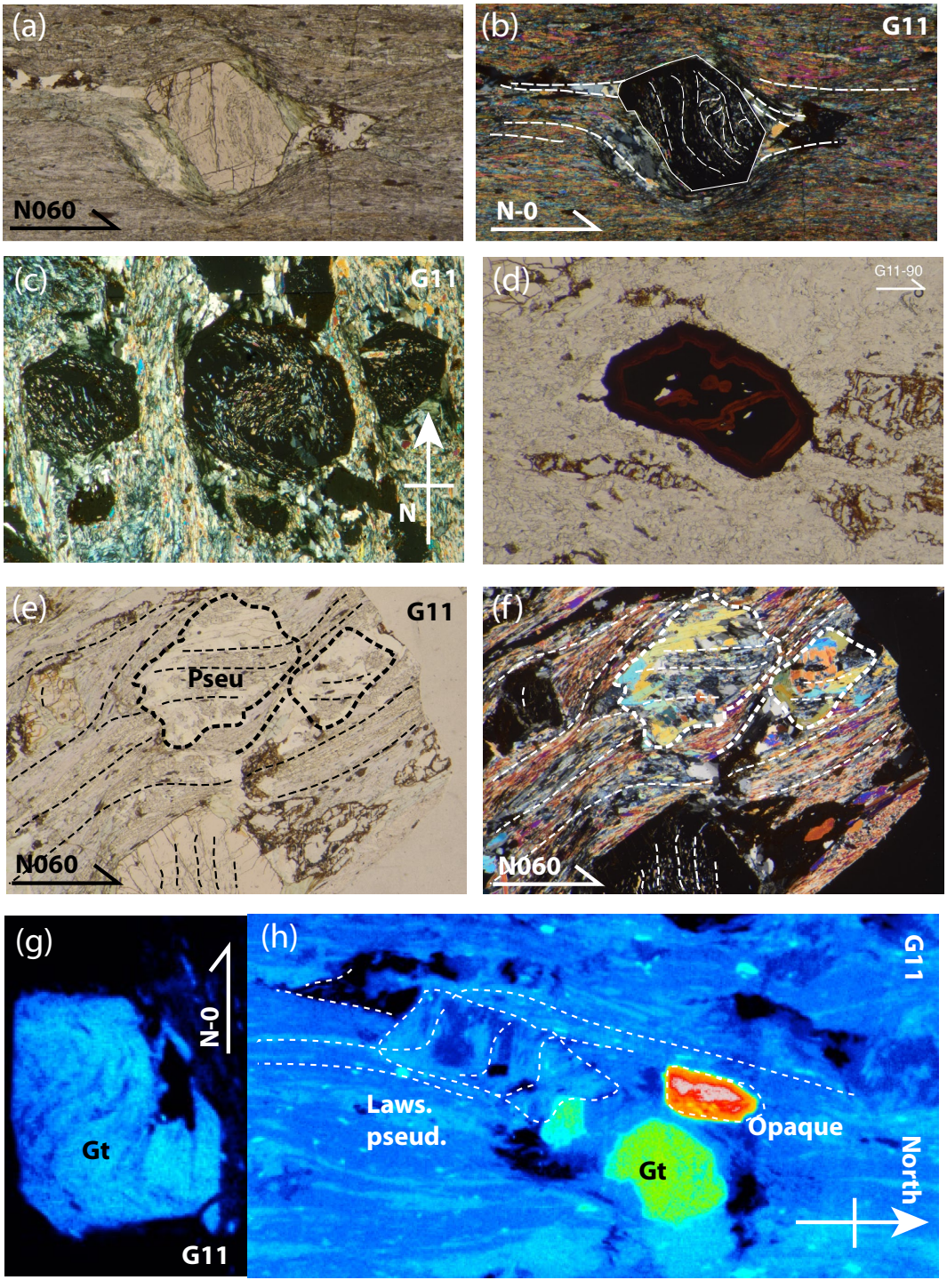

FIG. 5

https://doi.org/10.5194/se-2020-175
Preprint. Discussion started: 19 October 2020
© Author(s) 2020. CC BY 4.0 License.

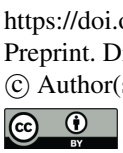

Solid Earth
Discussions
Open Access
EGU

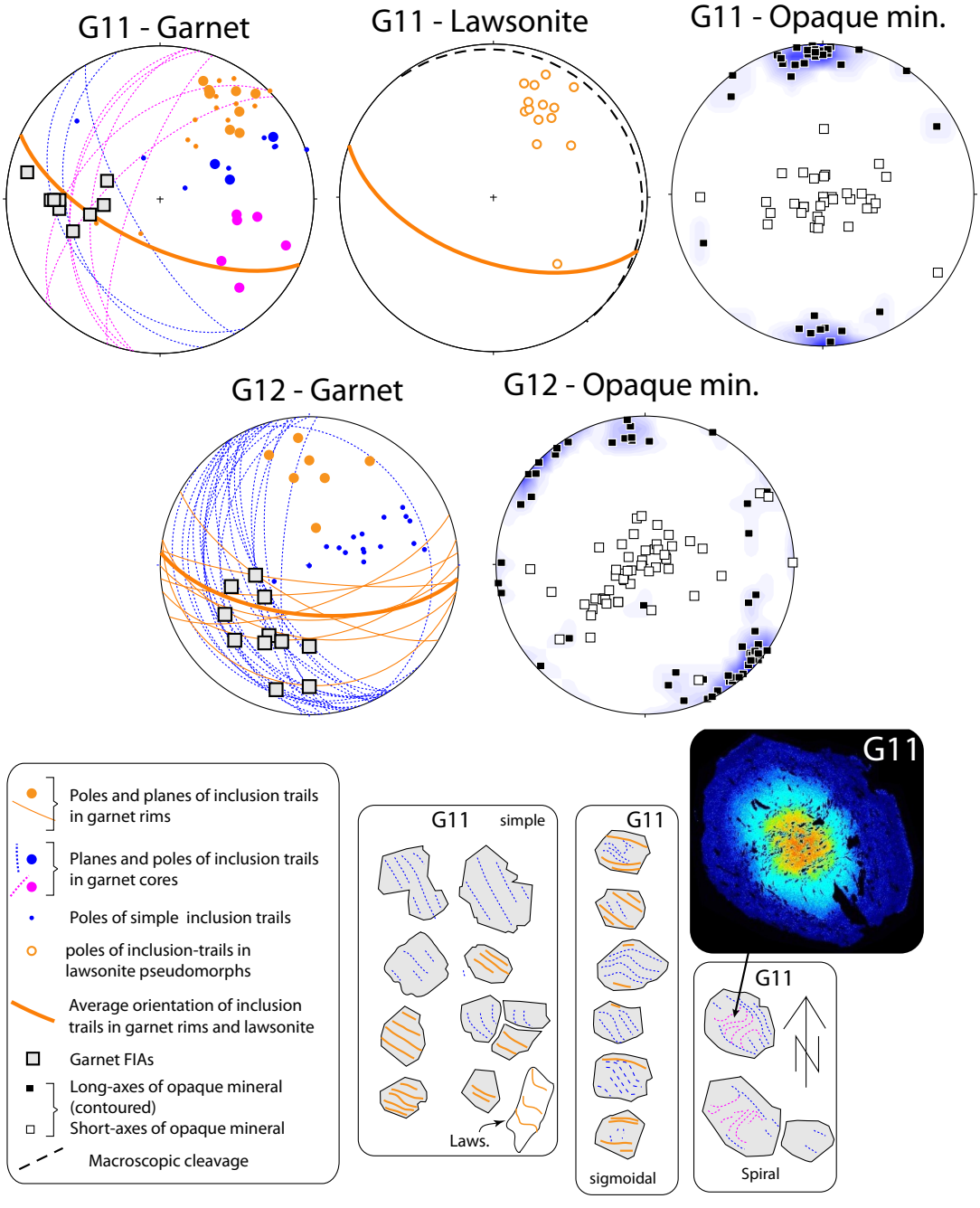

FIG. 6

https://doi.org/10.5194/se-2020-175
Preprint. Discussion started: 19 October 2020
© Author(s) 2020. CC BY 4.0 License.

Solid Earth
Discussions
Open Access
EGU

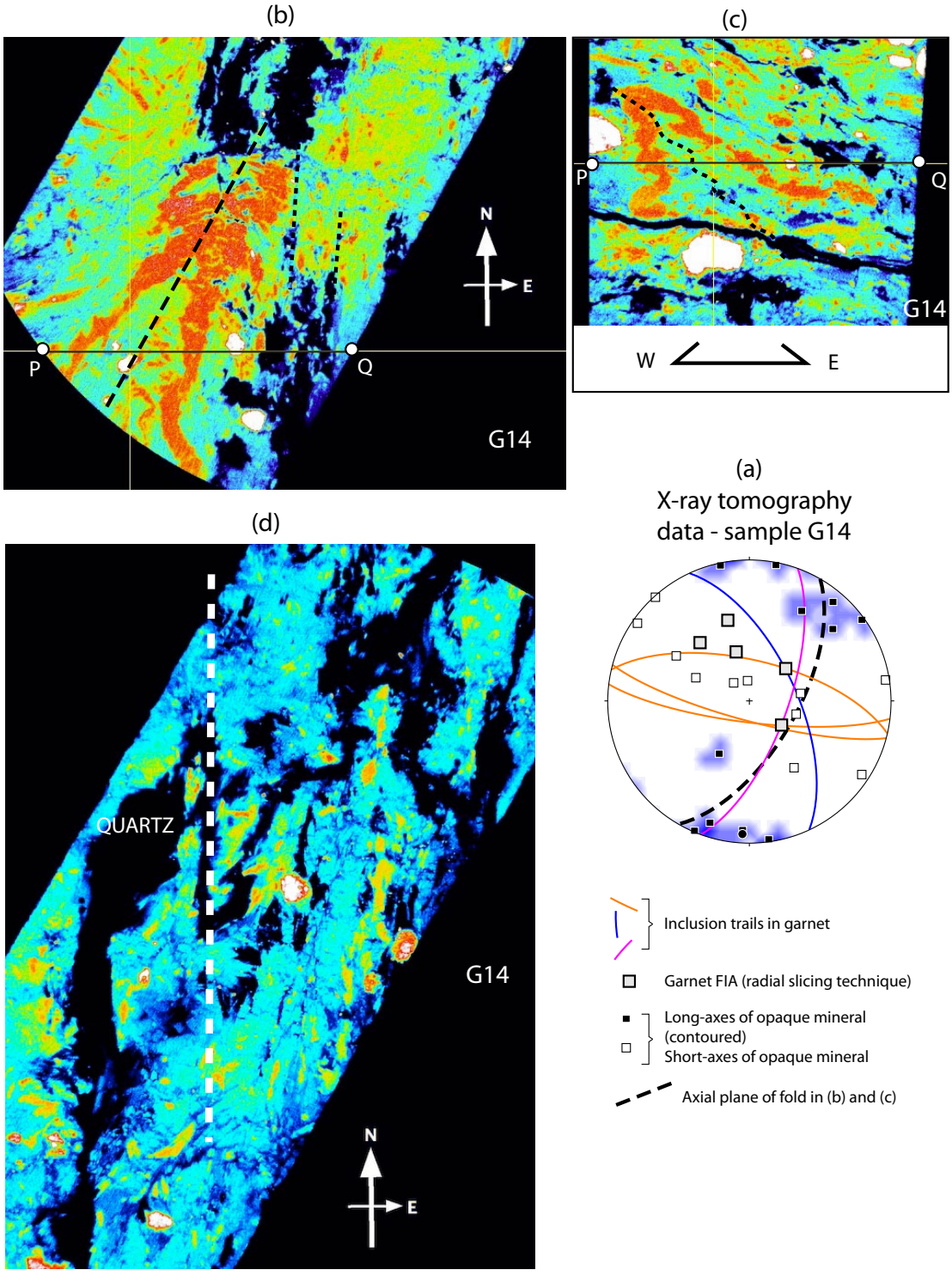

FIG. 7

https://doi.org/10.5194/se-2020-175
Preprint. Discussion started: 19 October 2020
© Author(s) 2020. CC BY 4.0 License.

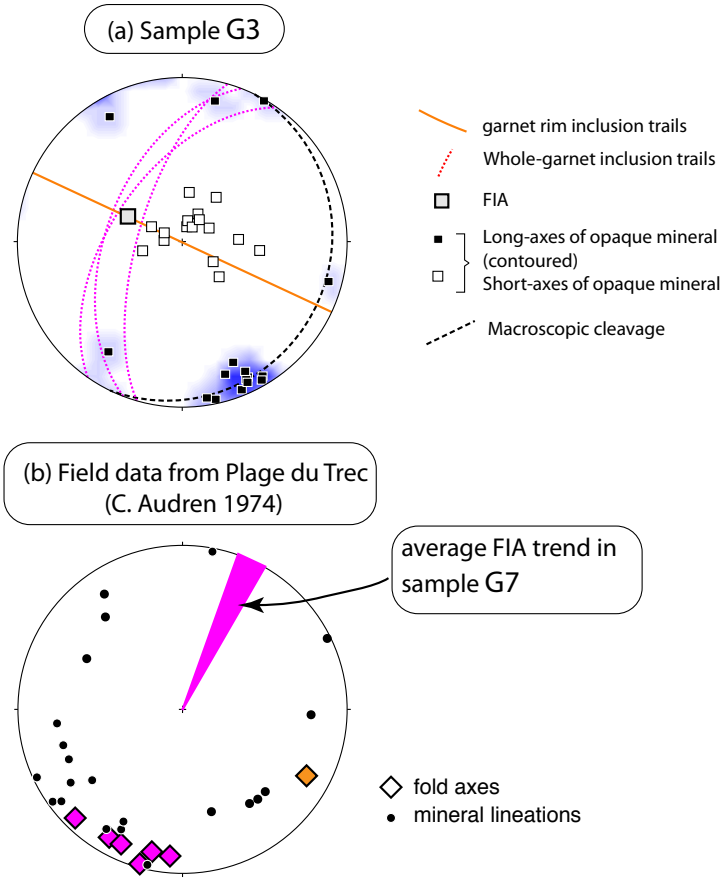

FIG. 8

https://doi.org/10.5194/se-2020-175
Preprint. Discussion started: 19 October 2020
© Author(s) 2020. CC BY 4.0 License.

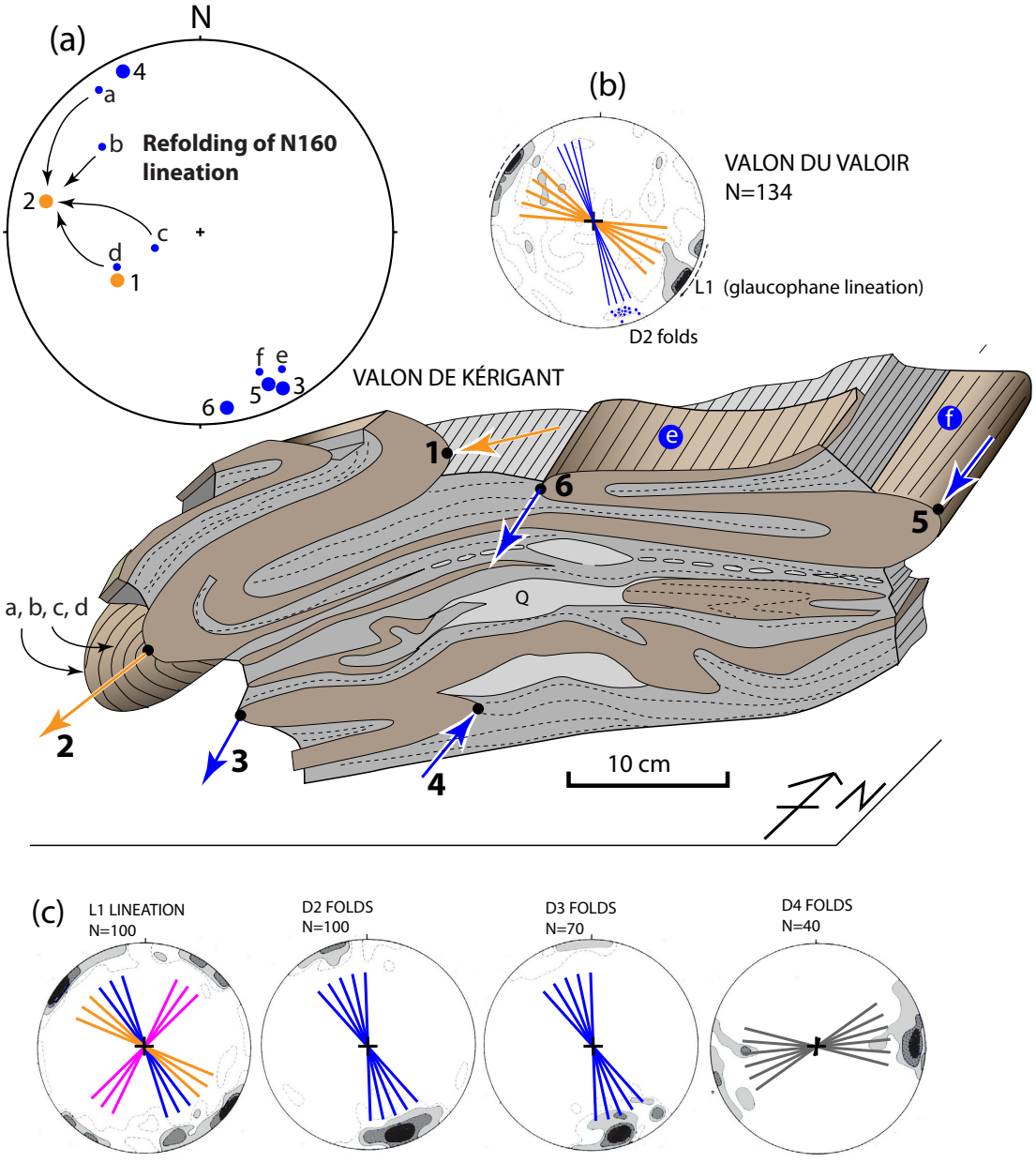

FIG. 9

https://doi.org/10.5194/se-2020-175
Preprint. Discussion started: 19 October 2020
© Author(s) 2020. CC BY 4.0 License.

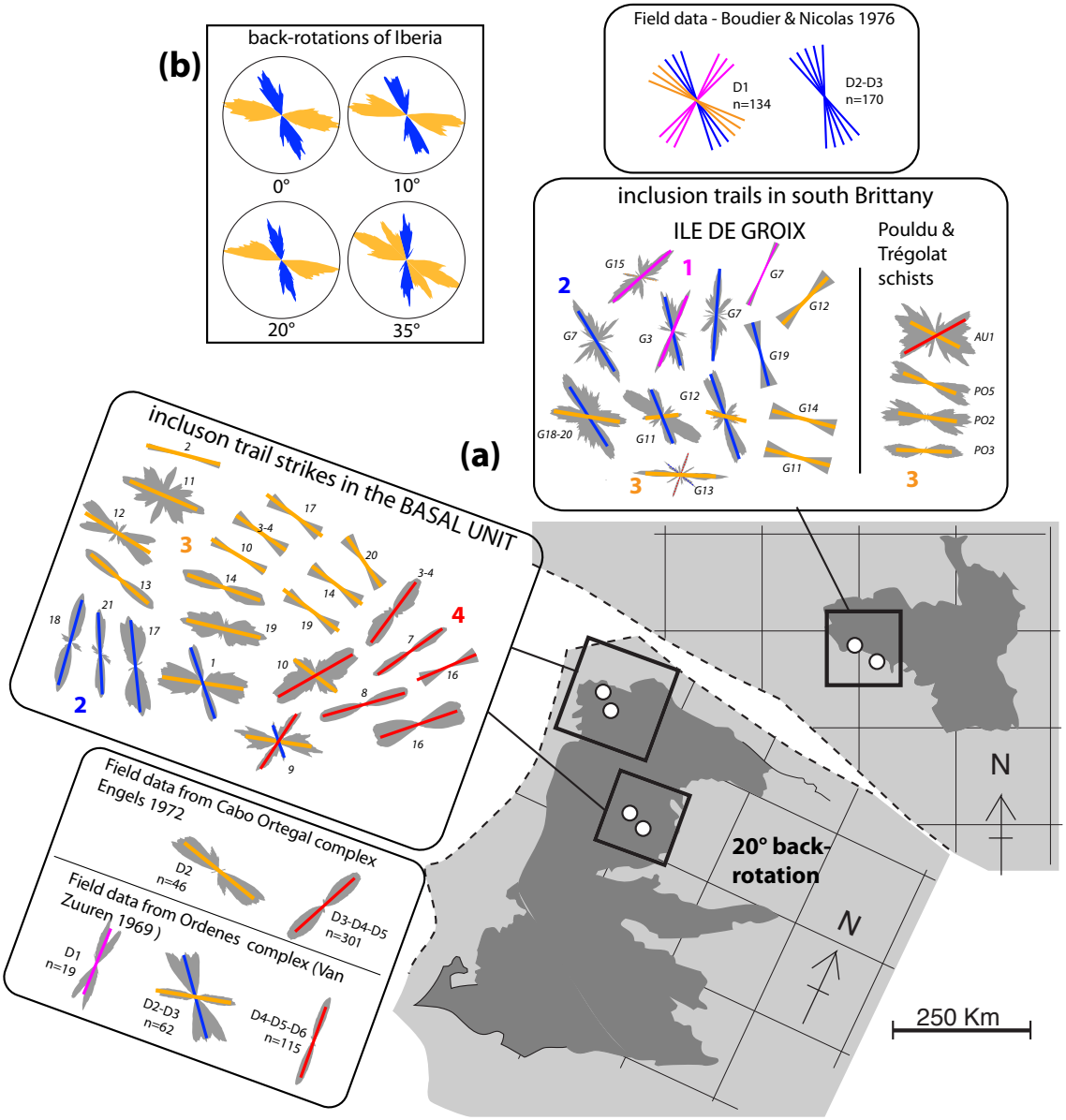

https://doi.org/10.5194/se-2020-175
Preprint. Discussion started: 19 October 2020
© Author(s) 2020. CC BY 4.0 License.

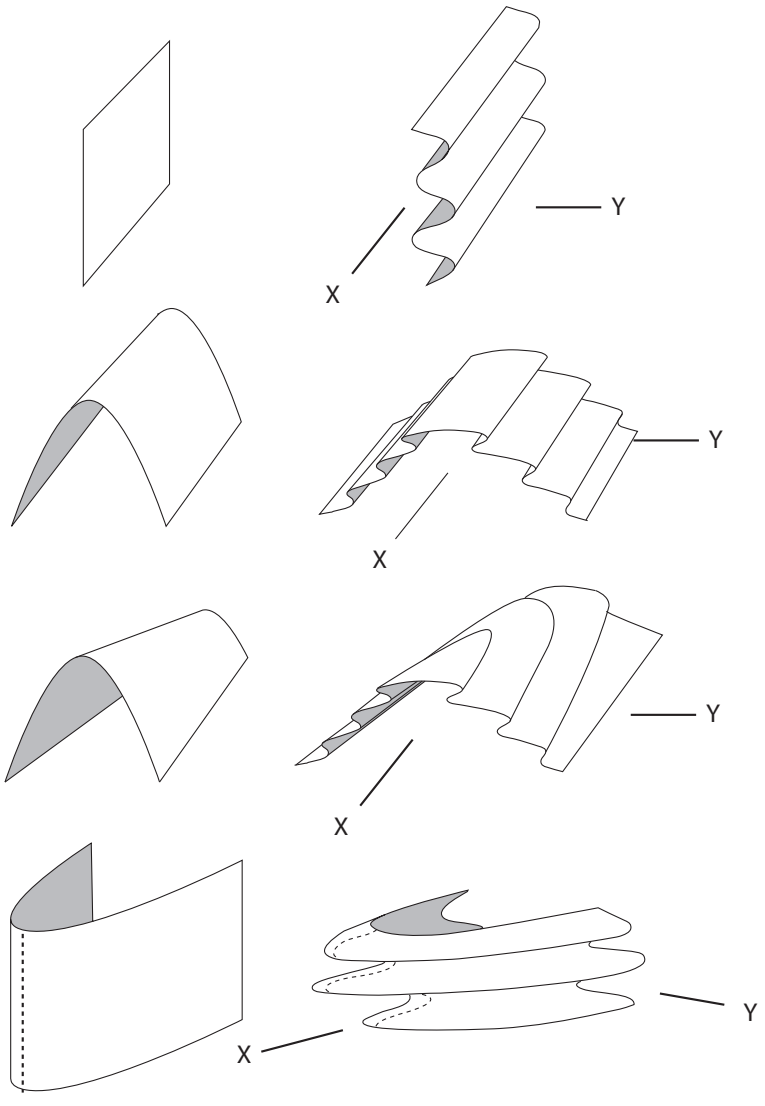

FIG. 11

https://doi.org/10.5194/se-2020-175
Preprint. Discussion started: 19 October 2020
© Author(s) 2020. CC BY 4.0 License.

Code/Data availability
All data are presented in the paper itself. No supplement is needed.

Author contributions
Aerden did the field work, conducted most of the research and wrote the manuscript
Sayab made and studied part of the thin sections.
Forde participated in part of the field work.
Ruiz-Fuentes studied part of the thin sections.

Competing interests
We have no competing interests